ELSEVIER

Polymer 41 (2000) 5513–5523

polymer

Phase separation induced by crystallization in blends of polycaprolactone and polystyrene: an investigation by etching and electron microscopy

H.M. Shabana[a,1], R.H. Olley[a,*], D.C. Bassett[a], B.-J. Jungnickel[b]

[a]*J.J. Thomson Physical Laboratory, Whiteknights, Reading RG6 6AF, UK*
[b]*Deutsches Kunststoff-Institut, D-64289, Darmstadt, Germany*

Received 14 June 1999; received in revised form 19 August 1999; accepted 29 September 1999

Abstract

Blends of ϵ-polycaprolactone (PCL) and low molecular weight atactic polystyrene (PS) are among those which show an upper critical solution temperature, and where one component (in this case PCL) is crystallizable, leading to several possible competitive interactions between blend decomposition and crystallization. Scanning and transmission electron microscopy have been used to obtain finer morphological information relating to two compositions where this phenomenon has already been followed under the optical microscope. This has been made possible by the development of several etchants which allow inspection of the internal bulk morphology with good resolution. The system 40% PCL–60% PS decomposes binodally to a majority phase with roughly equal proportions of PCL and PS surrounding blobs of a minority phase composed almost entirely of PS. The large spherulites of PCL grow around and engulf the PS-rich blobs. The system 60% PCL–40% PS crystallizes from a homogeneous melt. In this case, as the low molecular weight PS is able to diffuse outward from the growing spherulite, the composition of the remaining melt changes to one which can decompose binodally. TEM shows the PCL lamellae to be separated in bundles, as is found in other blend systems. The PS-rich phase is observed to segregate either at the spherulitic growth front, where it forms small droplets of the order of 1 μm in size, or outside the spherulites, where it coalesces into larger droplets, which in bulk specimens ooze to the surface giving a featureless layer largely concealing the spherulitic morphology. Spinodal decomposition has also been observed in melt which has been rapidly quenched in liquid nitrogen and allowed to warm up to room temperature.

Keywords: Polycaprolactone–polystyrene blends; Phase separation; Electron microscopy

1. Introduction

Although the specific characteristics of polycaprolactone (PCL) namely low melting point, mechanical weakness and solubility in a wide range of solvents, render it, as a material on its own, of little practical application, it does blend with a wide range of other polymers. Many authors have been trying to improve the properties of PCL by incorporation of a wide variety of other polymers, for example, poly(vinyl chloride) (PVC), phenoxy, polycarbonate, styrene-*co*-acrylonitrile (SAN) and polystyrene. This capacity for forming such a wide range of blends, both compatible and incompatible, makes PCL a favourite material for theoretical and fundamental blend studies. With polystyrene (PS), in which we are interested here, there are three main tracks along which PS can be induced to blend with PCL, firstly block copolymerization of PCL and PS [1], secondly blending PCL with styrene copolymer [2–4] or thirdly use of very low molecular weight PS or styrene oligomer [5–11].

With polystyrene the blends appear to show either mechanical compatibility or incompatibility, in that they exhibit a miscibility gap which intersects the (hypothetical) glass transition (T_g)-composition curve at two distinct compositions, with the corresponding T_g referring to two blend compositions, rather than those of the two pure components. Totally miscible blends show true compatibility in that they exhibit a single glass transition temperature, T_g, intermediate between that of either homopolymer. Blends of two crystallizable polymers such as PCL/polycarbonate [12] which are miscible in all proportions are rare, though this particular pair has been of interest as an anti-plasticizing modifier of epoxies [13]. More common are miscible pairs such as PCL/PVC, where only the PCL can crystallize, as spherulites which grow from the compatible

* Corresponding author. Tel.: +44-118-931-8572; fax: +44-118-975-0203.

E-mail address: r.h.olley@reading.ac.uk (R.H. Olley).

[1] Present address: Department of Physics, Faculty of Science, University of Mansoura, Egypt.

0032-3861/00/$ - see front matter
PII: S0032-3861(99)00713-2

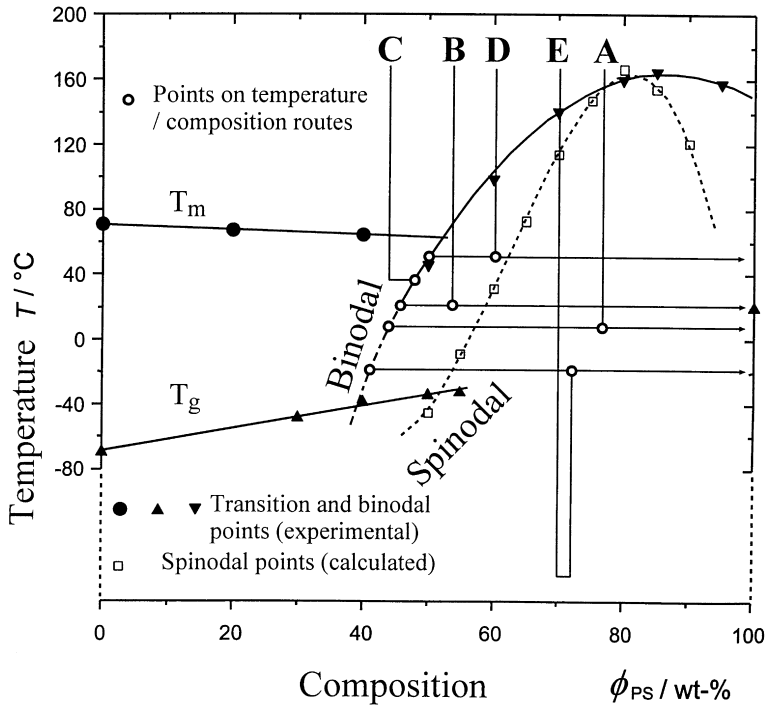

Fig. 1. Phase diagram of the system studied, showing five different routes of phase separation and crystallization.

mixture formed above its melting temperature. The miscibility of this blend is easily understood, since the ester-containing PCL is an electron donor while the halogenated PVC is an electron acceptor; even so, such a combination may not always be miscible, for example blends of poly(ethyl acrylate) with polyvinylidene fluoride [14]. In their investigation of PCL/PVC, Ong and Price [15] showed that up to about 50% PVC by weight, the samples were completely filled with spherulites composed of lamellae radiating from the centre. With increasing PVC content, the texture of the spherulites became coarser and more open. This system is one which illustrates particularly well the tendency for PCL in blends to grow as tightly banded spherulites [16], whereas those from pure PCL are only loosely banded, if at all. X-ray studies demonstrated that the PCL crystal structure was unaffected by the presence of PVC, suggesting that the PVC was contained within the spherulites but confined to interlamellar regions [17,18]. Other blends such as those of PCL with cellulosic polymers [19,20] may or may not exhibit true compatibility, dependent on their precise composition.

Of particular interest are blends containing PCL which display upper or lower critical solution temperatures near the temperature region where crystallization takes place. They are a prime example of semicrystalline–amorphous mixtures, in which there is a melting point curve in addition to the binodal and spinodal lines, and which can give a variety of possible phase diagrams [6]. Blends with SAN co-polymers are a much-studied example, showing how the phase separation and crystallization phenomena are very dependent on the composition of the SAN [3,21–23] and how phase separation can be driven by changes in composition as the PCL is withdrawn by crystallization from the mixture into the solid phase [4].

The present system, PCL with low molecular weight PS, is also one whose phase diagram has been investigated by many authors [7,24–26]. Tanaka and Nishi [5] were the first who demonstrated that this system has an upper critical solution temperature. They investigated the phase diagram by direct observation under a phase contrast microscope and a binodal line was determined, while the melting points of PCL spherulites in the mixture were determined both by microscopic observation under polarizing light and by differential scanning calorimetry (DSC). Burghardt has calculated [26] the phase diagram of systems exhibiting both crystallization and phase separation on the basis of Flory–Huggins theory. The phase diagram of these particular PCL/PS samples has been investigated by Jungnickel et al. [7] using turbidity measurements (binodal), Hoffman–Weeks treatment crystallization kinetics (melt/crystal equilibrium temperature), DSC (glass transition temperatures) and use of the Flory–Huggins equation with the value determined from melting point depression (spinodal).

When two or more non-equilibrium phenomena take place simultaneously, the final phases strongly depend on their dynamics and cannot be wholly determined by an equilibrium phase diagram. In the competition between crystallization and phase separation which occurs when quenching the material from the one phase melt region to a solidification temperature, four important cases (A–D) were distinguished [5], but a fifth (E) is also possible. These are drawn in Fig. 1, over the same phase diagram as in Ref. [7]:

(A) simultaneous spinodal decomposition and crystallization;
(B) simultaneous binodal decomposition and crystallization;
(C) crystallization-induced phase separation;
(D) separation-induced crystallization;
(E) quenching to an undecomposed glassy state, then on warming spinodal decomposition occurs leading to crystallization.

Further possibilities arise when performing the quench in two steps:

1. crystallization in an already binodally decomposed material;
2. crystallization in an already spinodally decomposed material.

Recently, Jungnickel and co-workers [7,27] have studied the same system to shed further light on the resulting structures according to the four routes (A)–(D), and to prove in more detail for this and other systems [14,28–30] the dependence of the resulting structure and the phase morphology on these routes and the relative rate of crystallization and phase separation, particularly in relation to the growth rate of the crystalline entities V_c and the rate of diffusion-driven migration of the amorphous material V_d [7]. In the extreme cases (1) where $V_c \gg V_d$ the released non-crystallizable component (NC) cannot escape from the growing spherulite and will be inserted between the crystallization lamellae; (2) $V_c \ll V_d$ the NC diffuses completely into the bulk melt, thus slowly increasing its concentration. After reaching the miscibility gap, the melt phase separates homogeneously and binodally. But in the intermediate case (3) where $V_c \approx V_d$, composition profiles develop around the growing spherulites. The binodal line will then be passed first at the spherulites' surfaces, where phase separation will start.

An X-ray study on the same system revealed that the amorphous regions between the lamellae within the PCL spherulites do not phase separate immediately on passing the binodal composition; instead, supersaturation of composition occurs. In their model [27], the initially bent lamellae flatten with time, and the supersaturated intra-spherulitic amorphous phase post-crystallizes according to the insertion crystallization scheme, whose thermodynamics have been discussed in detail [31] (actually development of subsidiary lamellae [32]) on a time scale that is comparable to the overall crystallization rate.

However, the architecture of spherulites is much more complex and requires more information than that given by a model of the lamellar structure alone. Taking this into consideration, there are (regardless of diffusion rates) three different spatial locations where the non-crystallizable component can be driven:

1. In interlamellar segregation, the amorphous blend component is rejected simply between the crystalline lamellae during the crystallization of PCL. This type of segregation is most hard to observe in real space, though a staining technique has revealed it in PCL/SAN blends [21].
2. In the so-called interfibrillar segregation, the amorphous component is segregated within the spherulites between stacks of lamellae. Isotactic–atactic polystyrene [33] has been claimed to exhibit this type of segregation; it has been observed directly in chlorinated polyethylene–PCL blends [34], by transmission electron microscopy (TEM) of sections relying on the mass contrast of the chlorinated component.
3. In interspherulitic segregation, the amorphous component is rejected at the envelope of the growing spherulite during the crystallization process. Such segregation has been observed in CPE/PCL blends at high contents of CPE and high crystallization temperatures [34], and in PCL–PS systems [5,7].

Most studies of blends have been carried out using combinations of X-ray scattering, neutron scattering, light scattering, thermal analysis and optical microscopy; published work studying the morphology of polymer blends by means of electron microscopy is small by comparison. Few electron microscope studies of this blend have been carried out so far, even though the real-space models used to interpret scattering are quite detailed, but the fine morphological details assumed cannot be detected by light microscopy [5,7]. So it was the purpose of this investigation to study in more detail, by means of electron microscopy, the structure of PCL/PS blends to obtain finer morphological information. In this crystallizable-amorphous system, we have attempted:

1. to find electron microscopic evidence about the location and the form of the non-crystallizable PS that has been released during the PCL crystallization; and
2. to ascertain the different morphologies produced in relation to different possible paths involving binodal or spinodal decomposition competing with crystallization.

In order to achieve this a method had to be developed for obtaining specimens appropriate for electron microscopy. This work describes the application of etching techniques [35] to sample preparation for both scanning and transmission electron microscopic examination, which reveal the structures arising from the different paths discussed above.

2. Experimental

2.1. Materials and methods

For the bulk specimens, blends of PCL (Union Carbide PCL 300, $M_w = 15\,000$, $M_n = 10\,000$) and atactic oligo-PS (Polymer Standard Service, $M_w = 840$, $M_n = 765$) were prepared from 5% by weight solution in tetrahydrofuran, stirring for 12 h at room temperature, evaporating the solvent and drying for 24 h at 60°C in vacuo [7,27]. Specimens

Table 1
Crystallization conditions for specimens

Specimen	Wt% PCL	Pre-treatment	Crystallization temperature (°C)	Crystallization time (days)
1	40	Homogenized at 160°C	46	25
2	40	Homogenized at 160°C, then decomposed for 3.5 h at 75°C	46	3
3	60	Homogenized at 90°C	44	7
4	60	Homogenized at 90°C	51	8
5	60	Homogenized at 90°C	51.2	20
6	60	Homogenized at 90°C	51	2

1 mm in thickness were given a pre-treatment to produce the desired liquid phase morphology then crystallized for the appropriate times and temperatures (details are given in Table 1).

The corresponding specimens for optical microscopy had a thickness of about 30 μm and were prepared immediately by solvent evaporation on a glass substrate. These film samples were (after removing them from the substrate) placed in the hot stage of a light microscope where further preparation (homogenization, crystallization, phase separation and so on) was performed.

2.2. Etching

Various etchant mixtures were developed for these blends, all based on a solution of potassium hydroxide in various alcohols, with or without added water, and sometimes containing cetyl trimethyl ammonium bromide (CETAB), of which the four compositions used in this blend study are given in Table 2. The particular alcoholic mixture in each case is that found by experience to give the best balance between revealing intricate detail and displaying the overall large scale structure (this varies between the different specimens), while the CETAB detergent was incorporated so as to improve the wetting of the surface and give greater uniformity of etching. The particular alcohol mixture would also partition into the chemically released oligo-PS, thereby reducing its T_g and viscosity, and it is variations in this factor which appear to determine whether the PS precipitates back onto the etched surface. The detergent action of CETAB does, however, appear to affect the manner in which any precipitated PS covers the surface.

Table 2
Etchants used

No.	Composition and time
1	800 mg KOH + 8 ml water + 14 ml *t*-butanol + 4 ml ethanediol[a] + 55 mg cetyl trimethylammonium bromide (CETAB), shaken for 5 h
2	2 g KOH + 10 ml ethanediol + 15 ml *t*-butanol, shaken for 4 h
3	150 mg KOH + 15 ml methanol, shaken for 1.5–8 min
4	500 mg KOH + 6 ml methanol + 6 ml water + 50 mg cetyl trimethylammonium bromide (CETAB), shaken for 30 min

[a] This small amount of ethanediol is necessary to prevent the mixture from separating into two phases.

2.3. Microscopy

Etched specimens were either coated with gold and examined under scanning electron microscopy (SEM), or replicated for TEM by a one-stage procedure. For this the sample was attached to a glass slide and the surface required to be replicated was uppermost. This surface was shadowed with tantalum–tungsten and coated with a carbon film. The polymer blend was solvent extracted, to leave the replica film on a copper grid for TEM. Since this is a direct replica, the image contrast has been reversed to give a more realistic impression of the morphology.

3. Results and discussion

The phase diagram of blends of polycaprolactone (PCL) and low molecular weight polystyrene (PS) shows an upper critical solution temperature (Fig. 1). It is not possible here to examine route A (spinodal decomposition) directly because even though one could choose a composition (approximately 20% PCL) which could be made to follow that route, the extreme mobility of the oligomeric PS would mean that the spinodally decomposed morphology would not be stable for any practical length of time. However, it might be possible to achieve this by rapid quenching to a very low temperature and allowing the decomposition to occur as the specimen slowly warms up to room temperature (route E in Fig. 1). This morphological development has, however, been followed in other systems by etching [36] and staining [21] techniques. The route D, of separation-induced crystallization, is of little relevance here.

The two compositions examined in this paper are:

1. The system 40% PCL–60% PS which decomposes binodally to a majority mixed phase of PCL and PS surrounding blobs of a minority phase composed almost entirely of PS. The two procedural variations are referred to as quenching routes B and 1 in the introduction.
2. The system 60% PCL–40% PS which crystallizes from an initially homogeneous melt, referred to as route C.

The crystallization of these two compositions has already

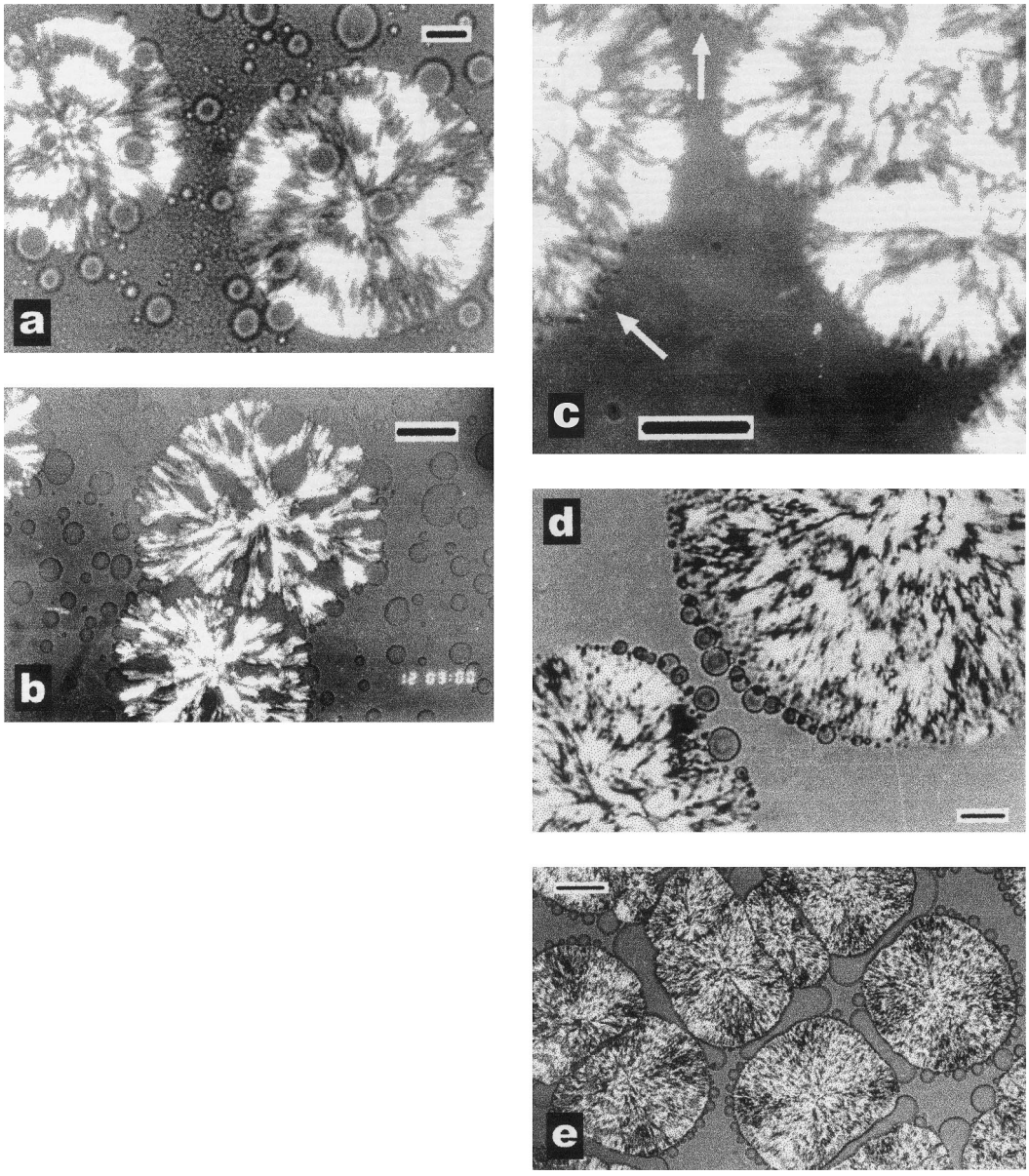

Fig. 2. Optical micrographs of: (a) 40% PCL, 40°C for 100 min, bar = 25 μm; (b) 40% PCL, 46°C for 27 h, bar = 100 μm; (c) 60% PCL grown at 44°C for 126 min, bar = 50 μm; (d) at 51°C for 109 h, bar = 25 μm; (e) at 51°C for 240 h, bar = 150 μm.

been followed under the optical microscope, for thin films [7]. Some of these results are presented in Fig. 2, which establish the equivalence of this and previous studies. It can be seen in Fig. 2a and b how the spherulites in 40% PCL grow round and engulf droplets of PS-rich phase. Since the droplets are already in place, the spherulite grows round them simply as if they were an inert "filler". In 60% PCL, at lower temperatures, Fig. 2c, the spherulites grow rapidly so that there is very little time for phase decomposition, and only small droplets are observed at the growth front of the spherulites. At higher temperatures a PS-rich phase separates at the growth front, Fig. 2d, starting at the points of closest approach of neighbouring spherulites but eventually occupying practically the entire volume of uncrystallized material, Fig. 2e. The present specimens were, in contrast, 1–2 mm in thickness, and while the PCL spherulitic morphology crystallized from these thicker specimens is similar to that seen in the previous optical work, there are additional effects observed due to their being three-dimensional. The top surfaces, and in some cases fracture surfaces through the specimens were examined after etching with a variety of etchants designed to attack the crystallizable PCL and (by different degrees) to disperse the non-crystallizable PS. During this work, two sources of PS were distinguished:

1. "phase-separated" PS: this is already separated in the crystallized sample and is not pure, but contains low molecular weight PCL;
2. "chemically released" PS, which is left after the PCL has been saponified by the etchant and dissolved away.

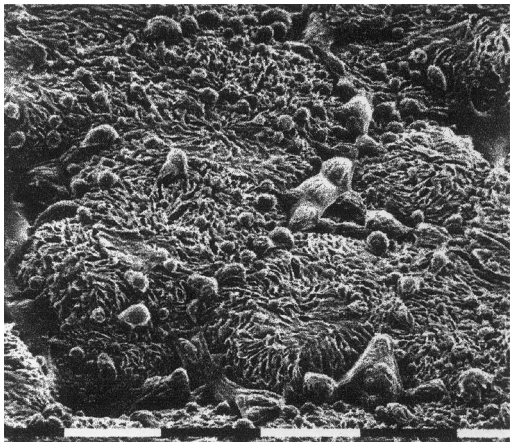

Fig. 3. SEM of specimen 1, treated with etchant #1. The PS-rich phase released from a homogenized melt is mostly driven to the large blobs at the boarders of the spherulites: bar = 0.1 mm.

In particular the PCL/PS system is very difficult to etch because on the one hand the crystallizable PCL is soluble in a wide range of media and has a low melting point, while on the other hand the incorporation of low molecular weight PS adds more difficulty to the etching process, since it is chemically resistant to the etching and also has a high mobility which enables the migration of PS to proceed faster. Since the PS is not broken down, it must go somewhere—either into the etching solution or to be deposited back on the surface of the specimen. Of the four methods which have been shown to work successfully with main-chain liquid crystalline polyesters [37,38], namely (1) permanganic etching, (2) acidic attack, (3) alkaline attack or saponification, and (4) attack with amines; the method of alkaline attack, in many variations, has been found generally to be much the best for PCL and its blends.

The etching formulation generally used (no. 1) was one which left the first kind of PS in situ where it occurred in the PS-rich phase, but generally dispersed the second type of PS released from the PCL-rich regions.

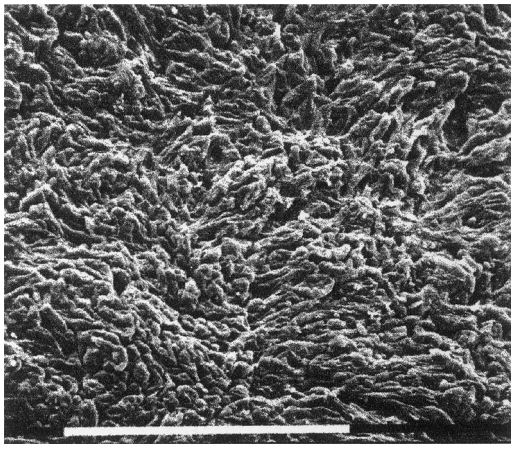

Fig. 4. SEM of specimen 2, treated with etchant #1. The PS-rich phase released from a decomposed melt is scattered as small blobs throughout the spherulites: bar = 0.1 mm.

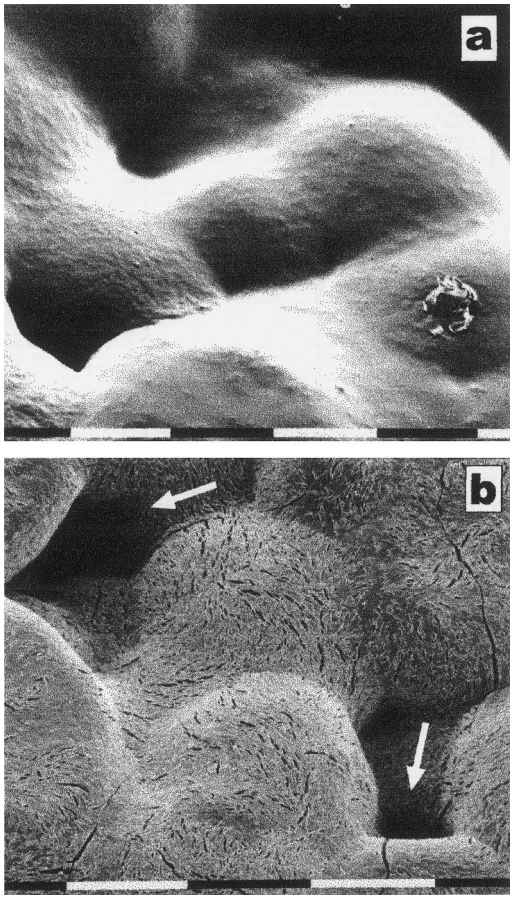

Fig. 5. SEM of specimen 3: (a) as received, covered with a layer of PS-rich phase; (b) after washing of this layer with methanol. Arrows indicate crevices formed in the last stages of crystallization as the remaining PCL-rich melt is withdrawn between the spherulites, bars = 0.1 mm.

3.1. The system 40% PCL–60% PS

This decomposes binodally to a majority phase with roughly equal proportions of PCL and PS surrounding blobs of a minority phase composed almost entirely of PS.

Two specimens from this system, crystallized at 46°C to completion of spherulite growth, were examined. Specimen 1 was crystallized from a melt previously homogenized above the clearing point, while specimen 2 was crystallized from one allowed to decompose binodally just above the melting point of the crystallizable PCL before being lowered to the crystallization temperature T_c. In specimen 1, Fig. 3 shows that a large part of the PS has been forced out at the edge of the growing spherulite into spherical droplets, with a smaller amount in droplets that were engulfed by the growing spherulite. Any PS which may have been trapped without phase separation in between lamellae in the amorphous part of the banded PCL spherulites has been dispersed by etchant no. 1 into the solution leaving the spherulitic

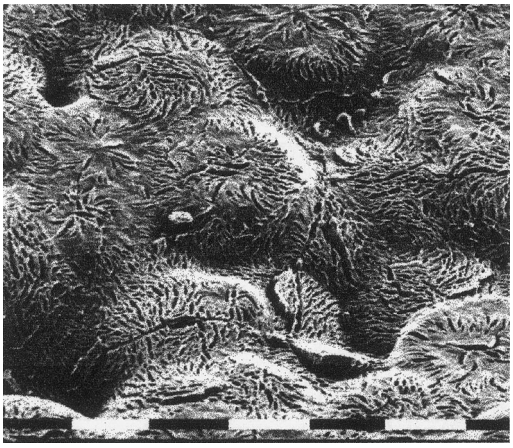

Fig. 6. SEM of specimen 3, treated with etchant #1. No phase-separated PS is seen: bar = 0.1 mm.

architecture clearly visible. In specimen 2, Fig. 4 shows how a large PCL spherulite has grown around and engulfed the previously formed PS-rich droplets. After etching with the same etchant these are left on the surface, partly obscuring the banded spherulitic morphology. This indicates that the inferences drawn from similar processes seen in thin films are also valid for truly three-dimensional specimens [7].

3.2. The system 60% PCL–40% PS

This forms a homogeneous melt. However, as the low molecular weight non-crystallizable PS is able to diffuse outward from the growing PCL spherulite, the composition of the remaining melt changes to one which can decompose binodally. At $T_c = 44°C$ (specimen 3), the PCL spherulites rapidly grow to impingement. Once binodal decomposition starts in the remaining regions of melt, the PS-rich phase migrates under the influence of gravity to the upper surface where it forms a featureless layer (Fig. 5a) which can be washed away with methanol, to reveal coarse banded spherulites (Fig. 5b). Note in this figure gulfs (arrowed) in the general surface where the last remaining PCL-rich melt has been pulled in by overall contraction as solidification proceeds. The PS-rich phase is inferred, from its infrared spectrum and easy washability with methanol, to contain a considerable proportion of low molecular weight PCL, also rejected from the crystalline phase because of its low molecular weight. In the corresponding thin film specimens, it was observed that once phase separation starts, small droplets appear at growth front of the spherulites (Fig. 2c, arrowed). In the confined geometry of a microscope slide, these could not migrate under gravity to the surface, and the question remained whether such droplets were engulfed by, and enclosed in, the growing spherulites. Since the melt composition inside the spherulitic architecture would have moved inside the binodal region before decomposition starts, it can also be questioned whether some binodal decomposition occurs within the spherulites, or whether some supersaturation remained there as concluded from SAXS [27]. After etching the bulk specimen 3 with etchant no. 1, which would disperse chemically released PS, no build-up of segregated PS is seen, either between or on the PCL spherulites (Fig. 6). These SEM results therefore militate against the idea that any phase-separated PS remains in the spherulite. Instead, it is driven away from the growing spherulite, and any excess remaining in the spherulites is likely to be held in a supersaturated composition.

With slower crystallization at $T_c = 51°C$, separation of the PS-rich phase is observed optically in thin films (Fig. 2d) to nucleate outside the spherulites, starting in regions of

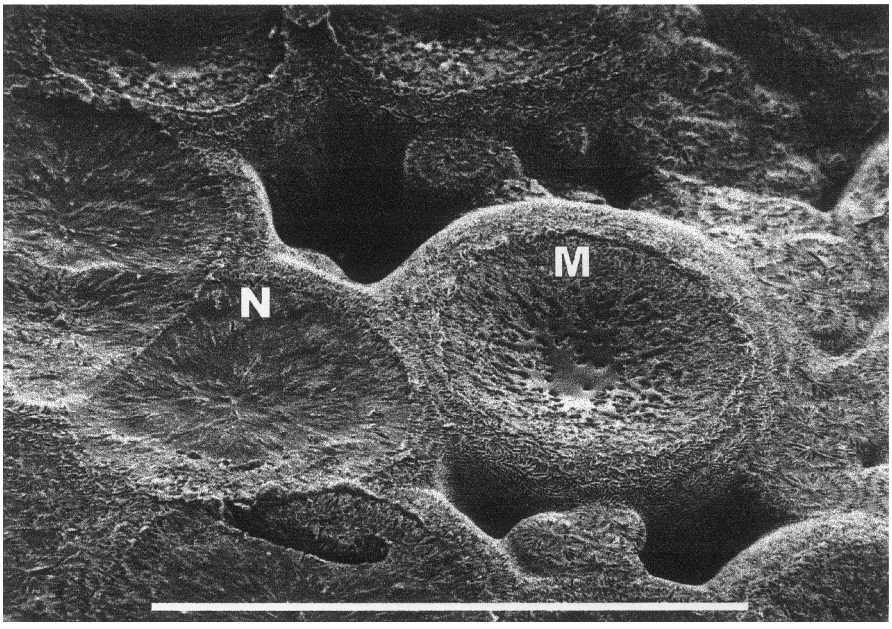

Fig. 7. SEM of specimen 4, treated with etchant #3. Some chemically released PS remains at the centre of spherulite M: bar = 0.1 mm.

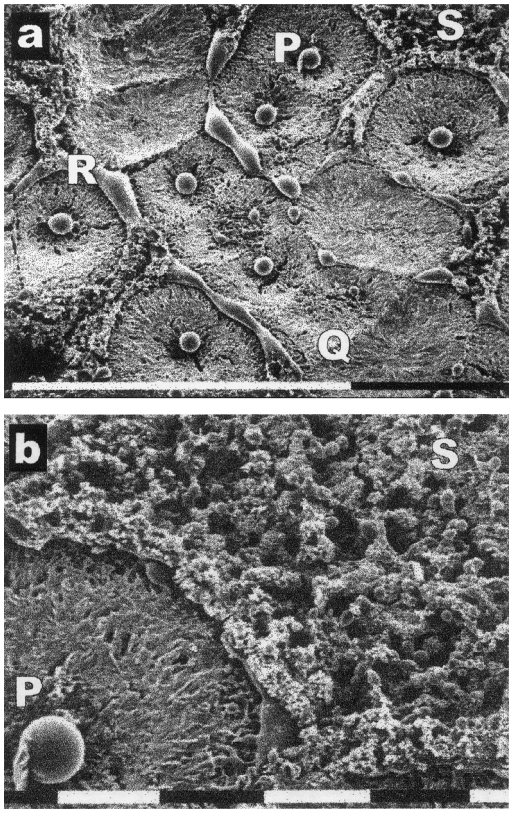

Fig. 8. SEM of specimen 4, treated with etchant #2: (a) showing P blobs of chemically released PS, Q early impingement of spherulites with no phase-separated PS, R late impingement with phase-separated PS, and S a region of remaining melt, crystallized on quenching, bar = 1 mm; (b) detail of P and S, bar = 0.1 mm.

closest approach, i.e. of highest PS concentration. Longer crystallization times are needed for the bulk specimens to reach an equivalent stage of development since the glass slides supporting the thin films tend to increase nucleation. Specimen 4 was quenched after 8 days, just at the onset of phase separation. Etching with the general etchant no.1 shows in Fig. 7 two large isothermally crystallized PCL spherulites including M and N. Each of these is surrounded by a banded halo produced on quenching, while to the right of M there are small spherulites grown independently in the quenched melt. At the centre of spherulite, M, the particular concave topography has unusually allowed intra-spherulitic polystyrene, released on etching, to settle on the surface instead of being dispersed into the etchant. Assisted by the detergent action of CETAB, it has wetted and spread over the surface. This spherulite has grown outwards from a nucleus well below the surface, but in the spherulite N, where the lamellae have grown directly outwards from the centre near the surface, PS has not precipitated. At M the outward-growing material at the centre appears to have been etched much faster, both giving the concave shape and releasing the PS more quickly, so that it cannot all be dispersed. PS released in this way cannot be washed away with cyclohexane, in contrast to the PS-rich phase segregated during crystallization and left in situ in other specimens, which is by its origin not pure PS, but contains a proportion of PCL, especially low molecular weight material. The boundaries of the isothermally crystallized spherulitic material in this location show a minuscule amount of PS released at the onset of phase separation, but in other areas where there are fewer spherulites this is not seen, since the locally available melt is greater in volume and the PS concentration had not increased to the point where it would released by phase separation.

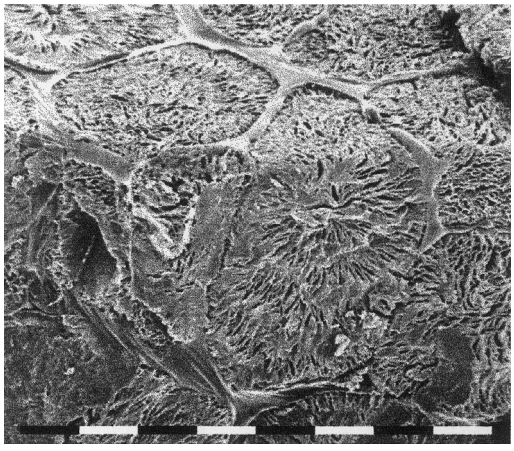

Fig. 9. SEM of specimen 5, treated with etchant #1, showing top and fracture surfaces, with phase-separated PS at inter-spherulite boundaries throughout the specimen: bar = 0.1 mm.

Etching the same specimen with etchant no. 2 reveals similar morphology, but the PS released chemically during etching tends to gather near its point of origin (Fig. 8a), since in the absence of CETAB it has not wetted the surface. So at P we see huge globules of PS at the centre of the PCL spherulites, in addition to the PS which was released at the spherulite boundaries in different amounts; Q shows early impingement (isothermal) with little build-up of PS, whereas R shows spherulites near impingement at quenching, with much build-up of PS, S shows an area far from impingement or quenching, with less build-up of PS. This is convincing evidence for concentration gradients forming near the boundaries of growing spherulites. Fig. 8b is a continuation of the top right of Fig. 8a, and shows small globules in quenched spherulites. These globules are of chemically released PS, and contrast with the pattern of PS globules in other parts of the specimen where spherulites have impinged during isothermal crystallization.

Specimen 5 was crystallized at 51°C for 20 days, which is enough time for much more binodal decomposition than in specimen 4. Throughout the depth of the specimen, the PS rich material has separated and accumulated between the spherulites which otherwise fill space. Fig. 9 shows both the top and the side surfaces of the specimen after treatment with etchant no. 1. The revealed location of PS is from the specimen itself and neither due to the surface topography nor due to the etchant which disperses any chemically

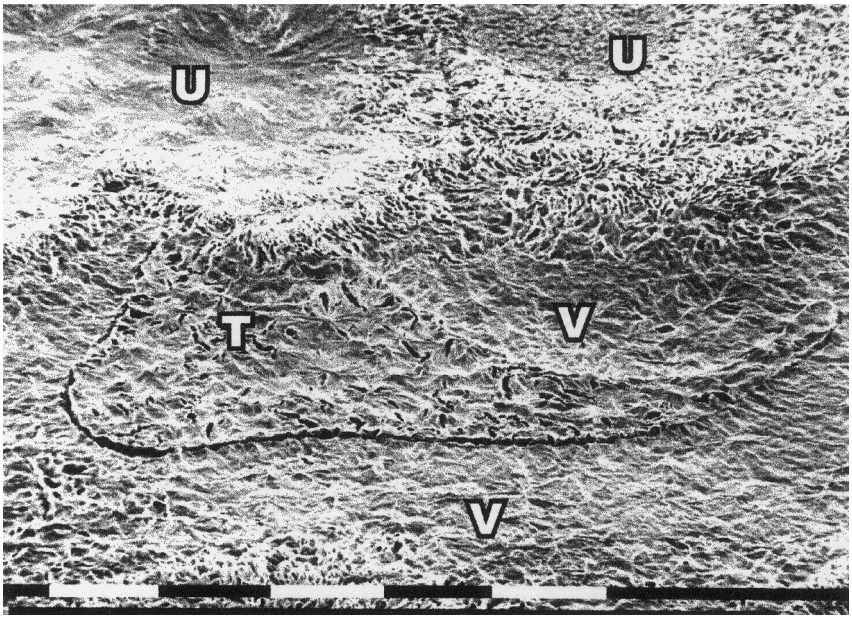

Fig. 10. SEM of specimen 5, treated with etchant #3, showing **T** an area of PS-rich phase in which the PCL has crystallized slowly after quenching **U** spherulites crystallized isothermally **V** areas on PCL-rich phase crystallized on quenching: bar = 0.1 mm.

released PS. However, as in specimen 2, the final remainder of the PS-rich phase had migrated to the upper surface, where it had formed a featureless layer, which could likewise be washed away with methanol. Nucleation density in this specimen was variable; some areas contained spherulites which impinged before phase separation started and others with limited amounts of PS-rich phase in between. Other areas, where there were fewer spherulites before quenching, contained pools of PS-rich melt which had been released from other parts of the specimen. These can best be seen using etchant no. 3, which after attack disperses the released PS to leave a clean surface as in Fig. 10. Such pools T, being isolated from the main spherulites U by the PCL-rich phase V, crystallize in the form of small independent spherulites. The PS-rich phase T does also contain some PCL which can crystallize as lamellae, a process observed optically in similar specimens over a period of 2 h after quenching.

The isothermal growth rate of spherulites was observed to remain reasonably constant [39], in spite of compositional changes, but this apparent constancy is essentially due to experimental limitations. Under the present conditions, the composition can change only between 40% PS (starting composition) and 50% (binodal composition), and the associated change in growth rate is within the experimental error [7]. After reaching the binodal, G drops remarkably [7]. This arises because the droplets must not only be displaced or engulfed (and occasionally deformed) but also they simultaneously grow. The displacement (or engulfing or deformation) force depends on the droplet's size, and increases with proceeding crystallization induced decomposition. This increase in its turn causes an additional time dependent decrease of spherulite's growth rate [40]. A legacy of this change is revealed by etchant no. 4 (Fig. 11a). This contains regions similar to those in Fig. 10, but surrounding the main PCL spherulites are rings which appear dark, where the material has grown under hindered conditions and has been etched away severely. This etchant also reveals that material growing upwards in a spherulite, from a nucleus well below the surface as in Fig. 11b, appears to be compartmented, which may be a phenomenon similar to the cellulation observed in branched polyethylenes [41]. It is to be noted that at this higher magnification a "dusting" of tiny globules is observable. These are of chemically released polystyrene which has precipitated on the surface.

Higher resolution observations were made under the TEM on replicas of an etched surface of specimen 5 prepared with etchant no. 1. These contained much detail, which tended to obscure the larger scale features which were more clearly displayed under the SEM. However, the higher resolution does show (Fig. 12) that lamellae are separated in bundles, not individually, corresponding to the situation in some isotactic–atactic PS blends [42]. This suggests that when interpreting scattering results, applying a model of interlamellar–interfibrillar–interspherulitic segregation [5,43] does have some basis in reality. Also it has been observed that, in the peripheral parts of the spherulites, where slow growth occurs through the separated front as discussed in the previous paragraph, the bundling of the lamellar texture is on a finer scale. In this specimen, therefore, there is evidence of four processes in the development in both crystallization and phase separation. These are:

1. isothermal growth before phase separation;
2. restricted isothermal growth after phase separation;

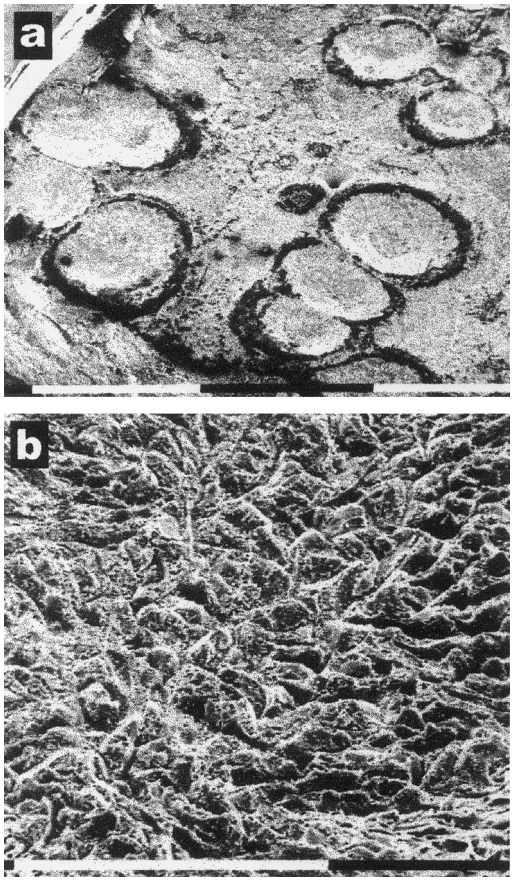

Fig. 11. SEM of specimen 5, treated with etchant #4: (a) showing spherulites crystallized isothermally with dark peripheries where phase-separation has started, bar = 0.1 mm; (b) detail of a spherulite centre showing compartmental structure and chemically released PS precipitated on the surface as tiny droplets, bar = 0.1 mm.

3. quenching of PS-rich melt surrounding PCL spherulites; and
4. quenching of isolated pools of PCL-rich melt.

One can therefore conclude that, the first system (40% PCL–60% PS) is phase-separated binodally, either prior to or coincidentally with crystallization, to a majority phase of PCL and PS, and a minority phase composed almost entirely of PS, and that this process is the dominant one in determining the final structure. On the other hand, the second (60% PCL–40% PS) crystallizes from a homogeneous melt and then phase separation is induced as PCL is removed from the melt by crystallization and regions whose composition falls within the binodal line are formed. Depending on the thermal treatment, crystallization and phase separation phenomenon may both take place simultaneously, or either crystallization induced phase separation or phase separation induced crystallization may dominate. There is no hard and fast line, but rather a gradual transition from one route to the other when changing the crystallization temperature and time.

Finally, it is possible that spinodal decomposition has occurred in specimen 6. This was crystallized at 51°C for 2 days, which would imply that most of its volume would still have been molten up to point when it was quenched in liquid nitrogen. Fig. 13a shows the surface of the specimen after washing with methanol. If spinodal decomposition has occurred on warming to room temperature, as in route E, Fig. 1, the matrix of this structure (light)

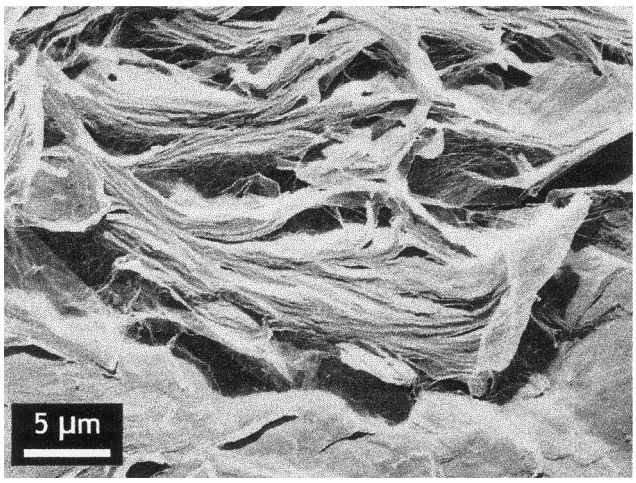

Fig. 12. Lamellar bundles are seen in detail under the TEM. Specimen 5, treated with etchant #1, direct replica, reverse contrast.

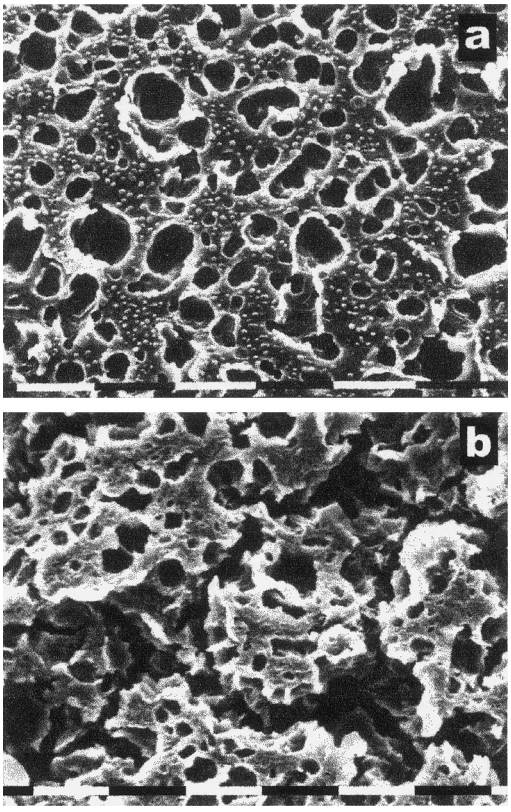

Fig. 13. SEM of specimen 6 showing spinodal structure: (a) the surface, washed with methanol; (b) treated with etchant #3, showing same structure in depth: bars = 10 μm.

would be polycaprolactone-rich, and would have been able to solidify at some temperature. This would have fixed the structure so that the PS-rich phase would have been confined to the tunnels (dark), from which, being of very low viscosity, it could have been washed out by the methanol. After etching with etchant 3, the tunnel structure is observed to continue below the surface (Fig. 13b). This was unexpected, since a composition of 60% PCL (approximating to C in the figure) should not have been able to reach the calculated spinodal line, but it may be that the spinodal is much closer to the binodal than expected, and the morphological evidence is very much in favour of this.

4. Conclusions

1. Etching and electron microscopy can be applied to blend systems based on polyesters, in addition to the polyolefin systems already studied. This gives support and additional information to previous optical and scattering work, by giving clear evidence of morphology in real space.
2. Several etchants have been developed for the system PCL–PS which allow differential effects to be studied at high resolution.
3. These techniques have been widely used to study crystallization phenomena as a function of thermal history. Now in addition blend demixing phenomena can be so studied.
4. During crystallization, PS is partly segregated and concentrated outside the spherulites, but a proportion remains trapped between the lamellae.
5. Electron microscopic examination allows a further distinction to be made in the location of the non-crystallizable PS: (a) that which is phase separated during the thermal treatment of the specimens; and (b) that contained in the PCL-rich phase which becomes chemically separated during etching after the PCL has been saponified.
6. The electron micrographs reveal features showing the five routes of development in both crystallization and phase separation:
   - isothermal growth before phase separation;
   - isothermal growth after phase separation;
   - quenching of PS-rich melt surrounding PCL spherulites;
   - quenched isolated pools of PCL-rich melt; and
   - spinodal decomposition on heating from the glass, followed by crystallization.

Acknowledgements

The authors thank Dr M. Stein of the Deutsches Kunststoff-Institut for the preparation of the specimens and the optical microscopy of Fig. 2.

References

[1] Heuschen J, Jerome R, Teyssié P. J Polym Sci Polym Phys Ed 1989;27:523.
[2] Fernandes AC, Barlow JW, Paul DR. J Appl Polym Sci 1986;32:5357.
[3] Schulze K, Kressler J, Kammer HW. Polymer 1993;34:3704.
[4] Li WG, Prudhomme RE. J Polym Sci Polym Phys Ed 1993;31:719.
[5] Tanaka H, Nishi T. Phys Rev Lett 1985;55:1102.
[6] Tanaka H, Nishi T. Phys Rev A 1989;39:783.
[7] Li Y, Stein M, Jungnickel B-J. Coll Polym Sci 1991;269:772.
[8] Nojima S, Jerashima Y, Ashida T. Polymer 1986;27:1007.
[9] Nojima S, Satoh K, Ashida T. Macromolecules 1991;24:942.
[10] Shibanov YD, Godovski YK. Coll Polym Sci 1985;263:202.
[11] Shibanov YD, Godovski YK. Progr Coll Polym Sci 1989;80:110.
[12] Hatzius K, Li Y, Werner M, Jungnickel B-J. Angew Makromol Chem 1996;243:177.
[13] Don TM, Bell JP, Narkis M. Polym Engng Sci 1996;36:2601.
[14] Li Y, Schneider L, Jungnickel B-J. Polym Networks Blends 1992;2:135.
[15] Ong CJ, Price FP. J Polym Sci Polym Symp 1978;63:45.
[16] Defieuw G, Groeninckx G, Reynaers H. Polym Commun 1989;30:267.
[17] Khambatta FB, Warner F, Russell TP, Stein RS. J Polym Sci Polym Phys Ed 1976;14:1391.
[18] Russell TP, Stein RS. J Polym Sci Polym Phys Ed 1983;21:999.
[19] Brode GL, Koleske JV. J Macromol Sci—Chem 1972;A6:1109.
[20] Vazqueztorres H, Cruzramos CA. J Appl Polym Sci 1994;54:1141.
[21] Svoboda P, Kressler J, Chiba T, Inoue T, Kammer HW. Macromolecules 1994;27:1154.
[22] Kressler J, Svoboda P, Inoue T. Polymer 1993;34:3225.
[23] Higashida N, Kressler J, Inoue T. Polymer 1995;36:2761.
[24] Endres B, Garbella RW, Wendorff JH. Coll Polym Sci 1985;263:361.
[25] Briber RM, Khoury F. Polymer 1987;28:38.
[26] Burghardt WR. Macromolecules 1989;22:2428.
[27] Li Y, Jungnickel BJ. Polymer 1993;34:9.
[28] Jungnickel BJ. Crystallization induced composition inhomogeneities in polymer blends. Current trends in polymer science, Research Trends, 2, 1997. p. 157.
[29] Wellscheid R, Wüst J, Jungnickel BJ. J Polym Sci Polym Phys Ed 1996;34:267.
[30] Wellscheid R, Wüst J, Jungnickel BJ. J Polym Sci Polym Phys Ed 1996;34:893.
[31] Elsner G, Riekel C, Zachmann H-G. Adv Polym Sci 1985;67:1.
[32] Bassett DC, Hodge AM, Olley RH. Faraday Dis R Soc Chem 1979;68:218.
[33] Warner FP, Macknight WJ, Stein RS. J Polym Sci Polym Phys Ed 1977;15:2113.
[34] Defieuw G, Groeninckx G, Reynaers H. Polymer 1989;30:595.
[35] Olley RH. Sci Prog Oxford 1986;70:17.
[36] Shabana HM, Guo W, Olley RH, Bassett DC. Polymer 1993;34:1313.
[37] Shabana HM, Olley RH, Bassett DC, Zachmann H-G. J Macromol Sci—Phys 1996;B35:691.
[38] Chu C-M, Wilkes GL. J Macromol Sci—Phys B 1974;10:551.
[39] Khoury F, Passaglia E. In: Hannay NB, editor. Treatise on solid state chemistry, 1976, chap. 6.
[40] Bartczak Z, Galeski A, Martuscelli E. Polym Engng Sci 1984;24:1155.
[41] El Maaty MIA, Bassett DC, Olley RH, Jääskeläinen P. Macromolecules 1998;31:7800.
[42] Vaughan AS, Bassett DC. In: Booth C, Price C, editors. Crystallization and morphology from comprehensive polymer science—the synthesis, characterization, reaction & applications of polymers. Vol. 2: Polymer properties, Oxford: Pergamon, 1989.
[43] Vanneste M, Groeninckx G. Polymer 1995;36:4253.